

# The dark matter distribution in disk galaxies

Annamaria Borriello<sup>1</sup> & Paolo Salucci<sup>1</sup>

(1) *International School of Advanced Studies SISSA-ISAS – Trieste, I*

5 February 2020

## ABSTRACT

We use high-quality optical rotation curves of 9 low-luminosity disk galaxies ( $-21.4 \leq M_I \leq -20.0$ ) to obtain the velocity profile of the surrounding dark matter halos. We find that they increase linearly with radius at least out to the stellar disk edge, implying that, over the entire region where the stars reside, the density of the dark halo is constant.

The properties of the halo mass structure found are similar to that claimed for a number of dwarf and low surface brightness galaxies, but provide a more substantial evidence of the discrepancy between the halo mass distribution predicted in standard cold dark matter scenario and those actually detected around galaxies. We find that the density profile proposed by Burkert (1995) reproduces the halo rotation curves, with halo central densities ( $\rho_0 \sim 1\text{--}4 \times 10^{-24} \text{ g cm}^{-3}$ ) and core radii ( $r_0 \sim 5\text{--}15 \text{ kpc}$ ) scaling as  $\rho_0 \propto r_0^{-2/3}$ .

**Key words:** cosmology: dark matter – galaxies: spiral

## 1 INTRODUCTION

Rotation curves (RCs) of disk galaxies are the best probe for dark matter (DM) on galactic scale. Notwithstanding the impressive amount of knowledge gathered in the past 20 years, some crucial aspects of the mass *distribution* remain unclear. In fact, it is still a matter of debate the actual density profile of dark halos and whether it is universal or related to some galaxy property, such as the total mass. This is so partly because such issues are intrinsically crucial and partly because it is often believed that a RC leads to a quite ambiguous information on the dark halo density distribution (e.g. van Albada et al. 1985). However, this argument is valid only for rotation curves of low spatial resolution, i.e. those with less than 2 independent measures per exponential thin disk length-scale  $R_D$ , as is the case with the great majority of HI rotation curves. This is because the galaxy structure parameters are especially sensitive to both the *amplitude* and the *shape* of the rotation curve in the region  $0 < r < R_D$ , (e.g. Blais-Ouellette et al., 1999) which corresponds to the region of the RC steepest rise.

No reliable mass model can be derived if such a region is poorly sampled and/or radio beam-biased.

Instead, in the case of high-quality *optical* RCs having tens of independent measurements in this critical region, the kinematics yields the halo mass distribution. Moreover, the investigation is further simplified by the fact that the dark matter is distributed according to the regime of Inner Baryon Dominance (Salucci and Persic, 1999a; Salucci et al., 1999): galaxies have a characteristic transition radius  $R_{IBD} \leq 2R_d \left( \frac{V_{opt}}{220 \text{ km/s}} \right)^{1.2}$  such that, for  $r \leq R_{IBD}$ , the luminous matter totally accounts for the mass distribution whereas, outside the transition, the DM *rapidly* becomes the only relevant dynamical component. Thus, a high-resolution rotation curve, in connection with reliable surface photometry, resolves the dark halo structure.

Since the dark component can be better traced when the disk contributes little to the dynamics, it is convenient to investigate DM-dominated objects, like dwarf and low surface brightness (LSB) galaxies. It is well known that the general outcome is the claim of dark halos with cores of constant density, that exclude steeply cusped density distributions (Flores & Primack, 1994; Moore, 1994; Burkert, 1995; Burkert & Silk, 1997; Kravtsov et al., 1998; McGaugh & de Blok, 1998; Stil, 1999). However, this general finding is 1) under the *caveat* that the low spatial resolution of the RCs does not bias the mass modelling, and 2) somewhat uncertain as result of the limited amount of kinematical data from which they have been obtained (see van den Bosch et al., 1999).

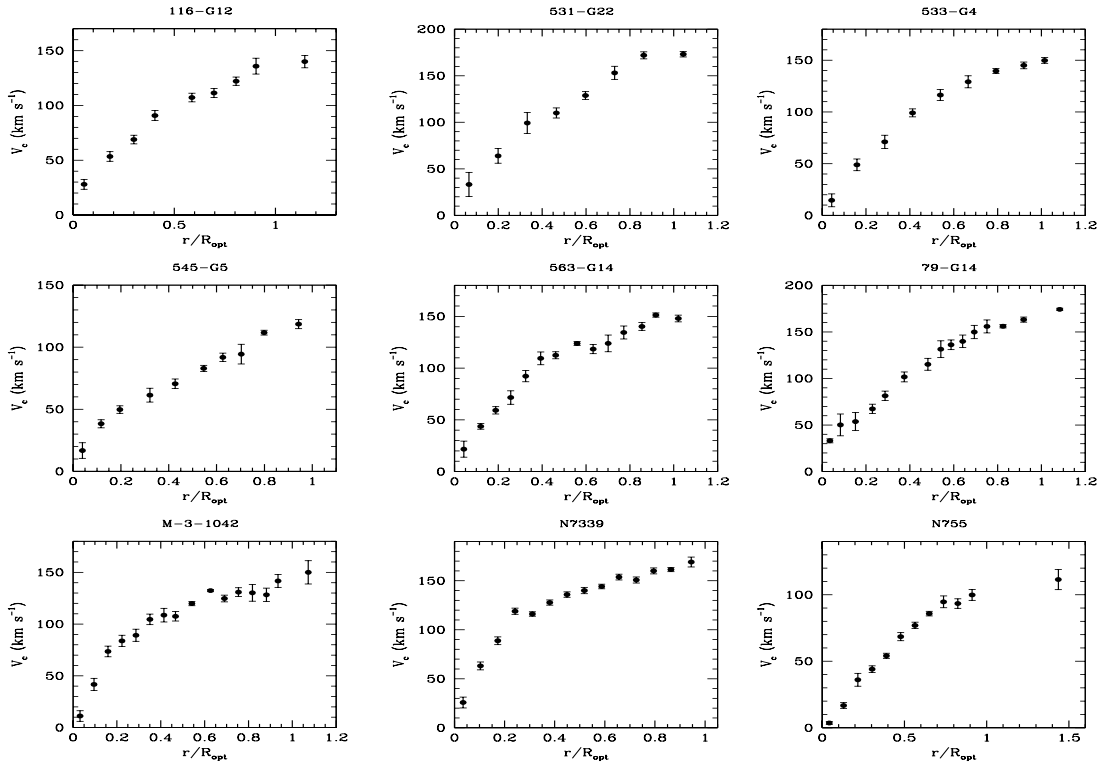
In this paper we will investigate the above-discussed issues by analysing a number of high-quality *optical* rotation curves extracted from Persic and Salucci (1995). The RCs of this sample are measured at an effective angular resolution of  $2''$ , which

arXiv:astro-ph/0001082v1 6 Jan 2000

**Table 1.** Observational properties of the sample galaxies

Galaxy	$R_D$ (kpc)	$V_{opt}$ (km s $^{-1}$ )	$M_I$
116-G12	1.7	133.5	-20.0
531-G22	3.3	171.1	-21.4
533-G4	2.7	151.1	-20.7
545-G5	2.4	124.4	-20.4
563-G14	2.0	148.9	-20.5
79-G14	3.9	167.1	-21.4
M-3-1042	1.5	148.0	-20.1
N7339	1.5	172.7	-20.6
N755	1.5	102.4	-20.1

(1) Galaxy name. (2) Length-scale of the exponential disk (from Persic & Salucci 1995), related to the optical radius  $R_{opt}$  (defined as the radius encompassing 83% of the light) by  $R_{opt} = 3.2R_D$ . (3) Circular velocity at  $R_{opt}$ . (4) Total  $I$ -band absolute magnitude (Mathewson, Ford & Buchhorn, 1992).

**Figure 1.** Rotation curves of the sample galaxies

corresponds to a spatial resolution of  $\sim 100(D/10 \text{ Mpc}) \text{ pc}$  which is  $\ll R_D$  for several nearby galaxies. In detail, we will select and then model a number of high-resolution rotation curves of bulge-less and low-luminosity galaxies. These objects, in which the stellar disk is the only baryonic component for  $r < R_{opt}$  and the dark halo is an important component at almost every radius, are the best opportunity to derive the DM halo velocity shape.

Since most of the properties of cosmological halos are claimed universal, it is worthwhile to concentrate on a small but particularly well suited sample of RCs in order to obtain the dark halo distribution around spirals with the minimum possible uncertainty. The systematics and the cosmic variance of the DM halo distribution will be investigated elsewhere (Salucci and Burkert, 1999; Salucci, 1999). Finally, let us stress that to establish the *actual* theoretical properties of CDM halos or to investigate *non standard* CDM scenarios possibly in agreement with observations is beyond the scope of this work.

In §2 we describe our sample of RCs. We present our mass modelling technique and its results in §3. In §4 we discuss the inferred halo profiles and their properties. We summarize our results in §5. Throughout this paper we adopt a Hubble constant of  $H_0 = 75 \text{ km s}^{-1} \text{ Mpc}^{-1}$ .

## 2 ROTATION CURVES

The rotation curves of the Persic & Salucci (PS95) ‘excellent’ subsample of 80 galaxies are all suitable for an accurate mass modelling. Indeed, these RCs properly trace the gravitational potential in that: 1) data extend at least to the optical radius, 2) they are smooth and symmetric, 3) they have small *rms*, 4) they have high spatial resolution and a homogeneous radial data coverage with  $\geq 30 - 100$  data points homogeneously distributed with radius and between the two arms. From this subsample we extract 9 rotation curves of galaxies of low luminosity with (almost) a perfect exponential *I*-band surface luminosity profile. These two last criteria, not indispensable for a successful *mass* decomposition, are however required to greatly minimize the uncertainties of the resulting dark halo *density* distribution.

The selected RCs are shown in Figure 1 (for all details we refer to PS95). They are still growing at  $R_{opt}$ , in that mostly tracing the dark halo component. Each RC has 8 – 18 velocity points inside  $R_{opt}$ , each one being the average of 2 – 6 independent data. The RC spatial resolution is better than  $1/20R_{opt}$ , the velocity *rms* is about 3% and the RCs logarithmic derivative is generally known within a uncertainty of about 0.05.

## 3 MASS MODELLING

We model the mass distribution in our spiral galaxies as the sum of two components: a stellar disk and a spherical dark halo. By assuming centrifugal equilibrium under the action of the gravitational potential, the observed circular velocity can be split into its two components:

$$V^2(r) = V_D^2(r) + V_H^2(r) \quad (1)$$

This is true as long as one assumes the gas in the galactic disk is in dynamic equilibrium. By selection, the stellar component is distributed like an exponential thin disk with an assumed radially constant mass-to-light ratio. In the r.h.s. of eq. (1) we can neglect the contribution from a gaseous disk, in that, for  $r \leq R_{opt}$ :  $V_{gas}^2(r) = (10^{-2} - 10^{-3})V_D^2(r)$  (Rhee & van Albada, 1996; Verheijen, 1997; Swaters, 1999). (Incidentally, this is not the case for HI RCs of dwarfs: most of their data are at radii where the gas contribution is relevant). We then write (Freeman, 1970):

$$V_D^2(r) = V_{opt}^2 \beta \frac{r^2}{R_{opt}^2} \frac{(I_0 K_0 - I_1 K_1)_{1.6r/R_{opt}}}{(I_0 K_0 - I_1 K_1)_{1.6}} \quad (2)$$

where  $I_n$  and  $K_n$  are the modified Bessel functions,  $V_{opt}$  is the measured circular velocity at  $R_{opt}$  and  $\beta \equiv \left(\frac{V_D^2}{V^2}\right)_{R_{opt}}$ . The parameter  $\beta$  varies from 0 to 1 and quantifies the contribution of the disk to the total circular velocity at  $R_{opt}$ . On the grounds of simplicity, we chose  $\beta$  as the disk free parameter rather than the disk mass-to-light ratio.

For the DM halo we assume a spherical distribution, whose contribution to the circular velocity  $V_H(r)$  is given by the functional form (Salucci, 1997):

$$V_H^2(r) = V_{opt}^2 (1 - \beta) (1 + a^2) \frac{x^2}{(x^2 + a^2)} \quad (3)$$

where  $x \equiv r/R_{opt}$  and  $a$  is the core radius measured in units of  $R_{opt}$ . The velocity profile of eq. (3) is neutral with respect to the mass-decomposition; in fact it can describe equally well a variety of mass models such as the maximum-disk, the solid-body, the no-halo, the all-halo, the CDM and, finally, the coreless-halo one. The actual values for  $a$  and  $\beta$  will discriminate the actual mass model.

Under the previous assumptions, the halo and the disk masses integrated up to a radius  $r$  are given by:

$$M_H(r) = G^{-1} V_H^2(r) r \quad (4)$$

$$M_D(r) = G^{-1} f^{-1}(r) V_D^2(r) r \quad (5)$$

$$f(r) = \frac{1}{2} \frac{r^3}{R_D^3} \frac{(I_0 K_0 - I_1 K_1)_{r/2R_D}}{1 - e^{-r/R_D} (1 + r/R_D)} \quad (6)$$

The free parameters  $\beta$  and  $a$  are determined by a  $\chi^2$ -minimization fit to the observed rotation curves:

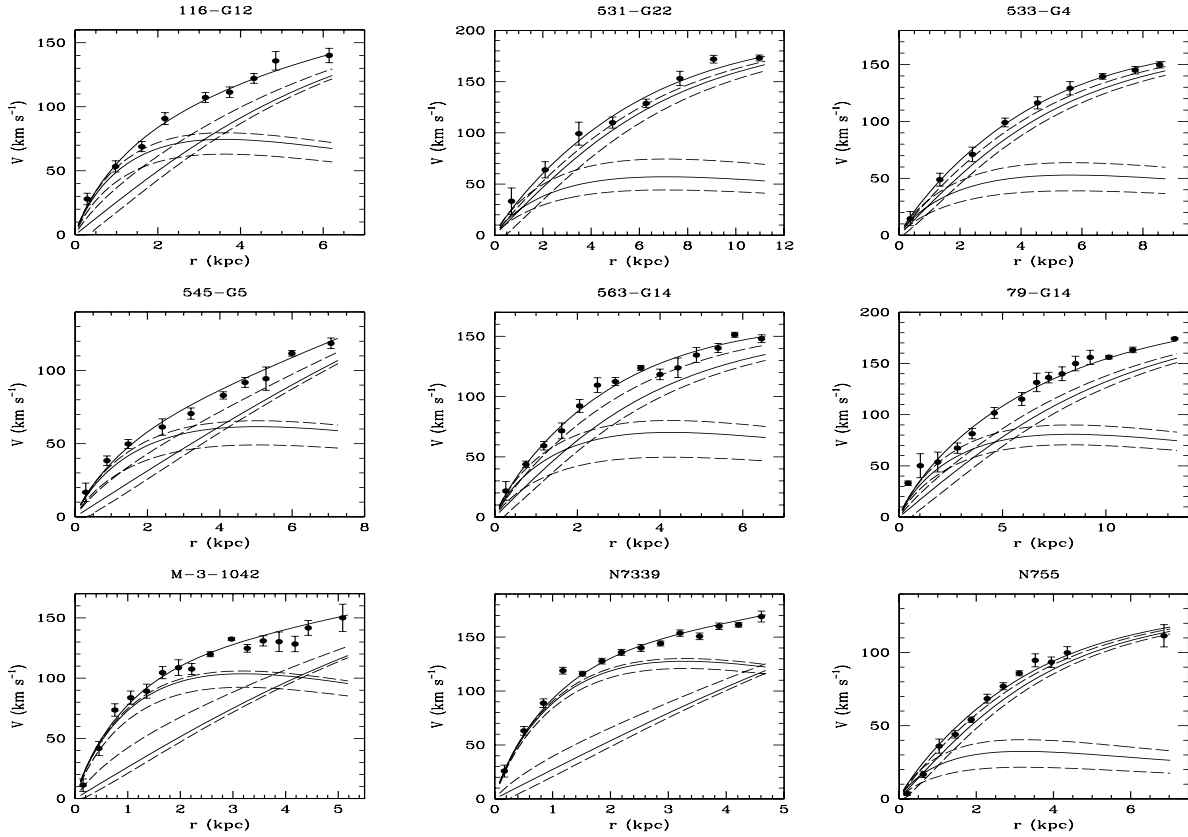
$$V_{model}^2(r; \beta, a) = V_D^2(r; \beta) + V_H^2(r; \beta, a) \quad (7)$$

A central role in discriminating among different mass decompositions is played by the derivative of the velocity field. It has been shown (e.g. Persic & Salucci, 1990b) that by taking into account the logarithmic gradient of the circular velocity field defined as:

$$\nabla \equiv \frac{d \log V(r)}{d \log r} \quad (8)$$

**Table 2.** Mass models

Galaxy	$\beta$	$a$	$M_D/L_I$
116-G12	$0.28^{+0.04}_{-0.08}$	$1.4^{+0.3}_{-0.2}$	$1.0^{+0.3}_{-0.3}$
531-G22	$0.10^{+0.07}_{-0.04}$	$0.8^{+0.8}_{-0.2}$	$0.3^{+0.05}_{-0.04}$
533-G4	$0.11^{+0.05}_{-0.05}$	$0.8^{+0.2}_{-0.1}$	$0.4^{+0.1}_{-0.1}$
545-G5	$0.22^{+0.03}_{-0.08}$	$2.5^{+0.5}_{-0.5}$	$0.7^{+0.1}_{-0.1}$
563-G14	$0.20^{+0.06}_{-0.10}$	$0.8^{+0.2}_{-0.2}$	$0.7^{+0.2}_{-0.2}$
79-G14	$0.21^{+0.05}_{-0.05}$	$1.0^{+0.1}_{-0.08}$	$0.7^{+0.1}_{-0.1}$
M-3-1042	$0.44^{+0.02}_{-0.09}$	$1.9^{+0.1}_{-1.1}$	$1.6^{+0.3}_{-0.4}$
N7339	$0.49^{+0.02}_{-0.05}$	$2.4^{+1.0}_{-0.7}$	$1.6^{+0.4}_{-0.4}$
N755	$0.09^{+0.05}_{-0.05}$	$1.0^{+0.1}_{-0.2}$	$0.2^{+0.04}_{-0.03}$

(1) Galaxy name; (2)-(3) Parameters of the best-fit model with their  $1\sigma$  uncertainties; (4) Disk mass-to-light ratio in the  $I$ -band in solar units.**Figure 2.** Mass modelling of the RCs (points with errorbars). The thick solid lines corresponds to the best-fitting models. The thin solid lines are the disk and the halo contributions. We also plot the maximum disk and the minimum disk models (dashed lines) for the disk and halo.

one can significantly increase the amount of information available from kinematics and stored in the shape of the rotation curve. We derive the parameters of the mass models by minimizing the generalized  $\chi^2_{tot}$ , defined as the sum of  $\chi^2$  calculated on both velocities and gradients:

$$\chi^2_{tot} = \chi^2_V + \chi^2_{\nabla} \quad (9)$$

$$\chi^2_V = \sum_{i=1}^{n_V} \frac{V_i - V_{model}(r_i; \beta, a)}{\delta V_i} \quad (10)$$

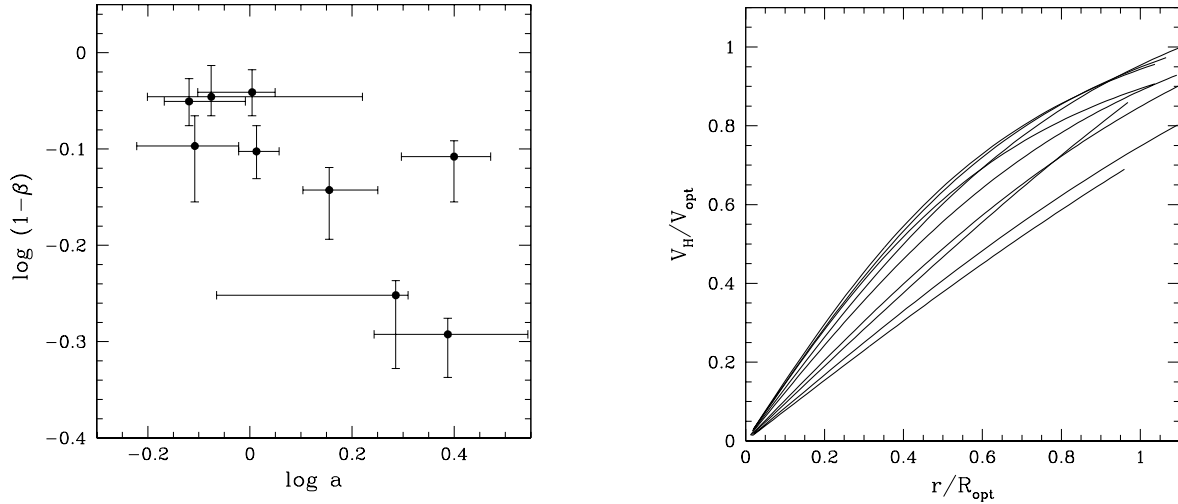


**Figure 3.** (left): relationship between the halo parameters,  $a$  is in units of  $R_{opt}$  (right): the halo velocity profiles of the sample galaxies.  $V_H(r)$  rises almost linearly with radius so that the DM density remains approximately constant.

$$\chi_{\nabla}^2 = \sum_{i=1}^{n_{\nabla}} \frac{\nabla(r_i) - \nabla_{model}(r_i; \beta, a)}{\delta \nabla_i} \quad (11)$$

where  $\nabla_{model}(r_i, \beta, a)$  is computed from eq. (2) – (3) and eq. (8). The generalized  $\chi_{tot}^2$  makes the mass model basically unique reducing the fitting uncertainty on  $\beta$  and  $a$ . The parameters of the best-fit models, derived through standard technique, are listed in Table 2, along with their  $1\sigma$  uncertainties. Indeed, the mass models are well specified: the allowed values for  $\beta$  and  $a$  span a small and continuous region of the  $(a, \beta)$  space. From eq. (1) and (2) we get a “lowest” and a “highest” halo velocity curve by subtracting from  $V(r)$  the maximum and the minimum disk contributions  $V_D(r)$  obtained by substituting in eq. (2)  $\beta$  with  $\beta_{best} + \delta\beta$  and  $\beta_{best} - \delta\beta$ , respectively.

The derived mass models are shown in Figure 2, alongside with the separate disk and halo contributions. It is then obvious that the halo curve is steadily increasing, almost linearly. The disk-contribution  $\beta$  and the halo core radius  $a$  span a range from 0.1 to 0.5 and from 0.8 to 2.5, respectively. The substantial uniqueness of the halo velocity best-model can be realized by noticing that the maximum-disk and minimum-disk halo velocity almost coincide.

In Figure 3 we show the correlation between the halo parameters: halos more dynamically important within  $R_{opt}$  (i.e. with higher  $1 - \beta$ ) have smaller core radii. Part of the scatter of the relation may arise because the sample is limited in statistics and in luminosity range (see Salucci and Burkert, 1999). Remarkably, we find  $a \geq 1$ : implying that the size of the halo velocity core extends beyond the disk edge (and the region investigated).

Although the present sample, by selection itself, is not the best suited to determine the disk mass-to-light ratio, it is useful to report that  $M_D/L_I$  ranges between 0.2 and 1.5 in solar units (see Tab. 2), that is between typical values of late-type spirals of similar luminosity (see Fig 2 in Salucci & Persic 1999a). It is worth to stress that, from a technical point of view, the present analysis computes the mass-to-light ratios from the model parameters as secondary quantities; the mass-to-light uncertainties in Tab. 2 do not indicate the goodness of the *halo* mass model, but only specify how well we know the *disk mass*.

## 4 DISCUSSION

In Figure 3 we report the halo velocity profiles for the nine galaxies. The halo circular velocities are normalized to their values at  $R_{opt}$  and expressed as a function of the normalized radius  $r/R_{opt}$ . These normalizations allow a meaningful comparison between halos of different mass: the radius scaling removes the intrinsic dependence of size on mass (more massive halos are bigger), whereas the velocity scaling takes into account that more luminous galaxies have higher circular velocities. It is then evident that the halo circular velocity, in every galaxy, rises almost linearly with radius, at least out to the disk edge:

$$V_H(r) \propto r \quad 0.05R_{opt} \lesssim r \lesssim R_{opt} \quad (12)$$

This implies that disk galaxies are embedded (inside  $R_{opt}$ ) in a *single* dark halo. In fact, if more dark halos were relevantly present, then, in order to not violate eq. (12), each of them should have a solid body velocity profile.

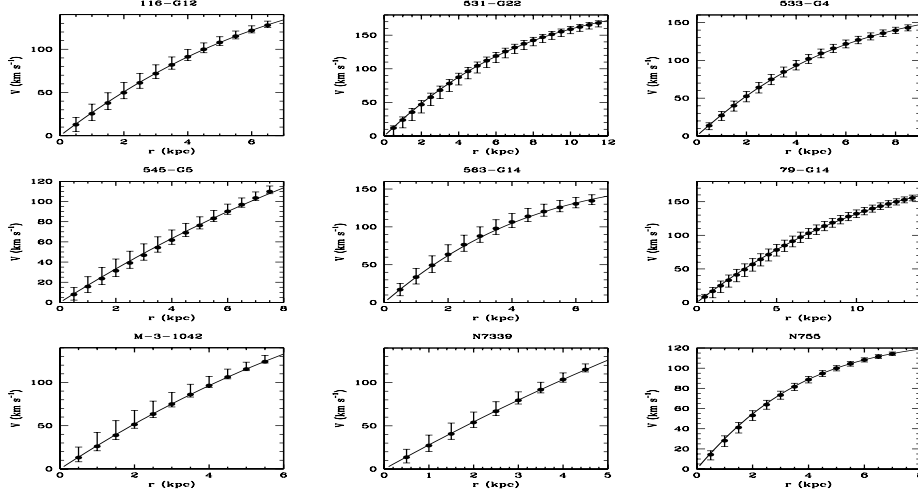


**Figure 4.** Halo velocities of the derived mass models (points with errorbars) fitted by the Burkert profiles (continuous lines).

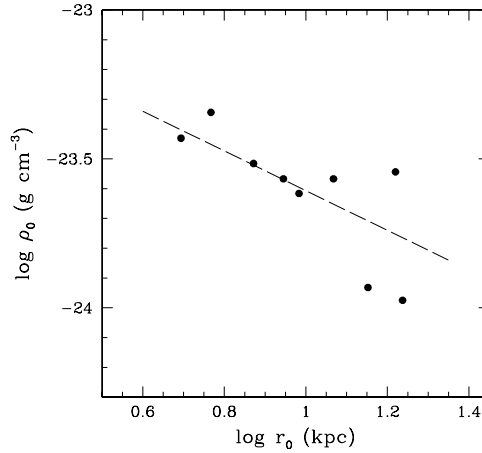


**Figure 5.** The parameters  $\rho_0$  and  $r_0$  of the Burkert mass models for the nine galaxies. The dashed line is the relationship  $\rho_0 \sim r_0^{-2.3}$  found by Burkert (1995) for dwarf galaxies.

The halo density profile has a well defined core radius within which the density is approximately constant. This is inconsistent with the singular halo density distribution emerging in the Cold Dark Matter (CDM) scenario of halo formation (Navarro, Frenk & White (NFW) 1996, 1997; Cole & Lacey, 1997; Tormen et al., 1997; Tissera & Dominguez-Tenreiro, 1998; Nusser & Sheth, 1999). In fact, especially if one considers that the CDM halos are, at small radii, even more cuspy than the  $r^{-1}$  profile (Fukushige & Makino, 1997; Moore et al., 1998; Jing, 1999; Jing & Suto, 1999; Ghigna et al., 1999), one should expect, at most:  $V_{CDM}(r) \propto r^{1/4}$ , instead of eq. (12). Let us stress that the halo properties of eq. (12) make it quite irrelevant, when we compare theory and observations, arguments, *per se* crucial, such as the CDM halos cosmic variance, its concentration parameter actual value or the effects of baryonic infalls or outflows (e.g. Martin, 1999; Gelato & Sommer-Larsen, 1999). The seemingly general halo property found raises an issue by itself.

Burkert (1995) has proposed the following phenomenological density profile:

$$\rho_B(r) = \frac{\rho_0 r_0^3}{(r + r_0)(r^2 + r_0^2)} \quad (13)$$

where  $\rho_0$  (the central density) and  $r_0$  (the scale radius) are free parameters. This density law has a core radius similar to that of the pseudo-isothermal density profile (e.g. Begeman, Broeils & Sanders, 1991), whereas, at large radii,  $\rho_B(r)$  converges to the NFW profile. Noticeably, the two parameters  $\rho_0$  and  $r_0$  are correlated  $\rho_0 \sim r_0^{-2/3}$ , so that the halo profiles reduce to a one-parameter family of curves.

We find that  $\rho_B(r)$  well reproduces our halo velocity profiles over the available radial range, namely out to  $R_{opt}$  (see Figure 4). In Figure 5  $\rho_0$  vs.  $r_0$  are plotted. Taking in consideration that typical uncertainties on  $\rho_0$  and  $r_0$  are about 0.15 dex and 0.07 dex, respectively, we confirm, with our sample, the structure relation found by Burkert for 5 dwarf galaxies.

## 5 SUMMARY AND CONCLUSIONS

We have performed the disk–halo decomposition for a well suited sample of 9 bulge–less disk galaxies with  $100 \leq V_{opt} \leq 170$  km s<sup>-1</sup>. These galaxies have a relevant amount of dark matter, so that the contribution of the luminous matter to the dynamics is generally small and it can be properly taken into account. In fact, the high spatial resolution of the available rotation curves allows us to disentangle the dark and luminous contributions from the total gravitational potential and therefore to derive the halo velocity profiles in a model independent way. We find that dark matter halos have a constant central density region whose size exceeds the stellar disk scale.

These halo rotation profiles disagree with the cuspy density distribution typical of CDM halos (e.g. Navarro, Frenk & White, 1997; Kravtsov et al., 1998). Indeed, the halo velocities can be very well described by means of the Burkert profile, an empirical functional form whose two structure parameters (central density and core radius) are related through:  $\rho_0 \sim r_0^{-2/3}$ .

This work is complementary to that of Salucci (1999) in which the halo velocity profile *at the disk edge* of 140 spirals of different luminosity:  $0.75 \leq d \log V_H(r)/d \log r|_{R_{opt}} \leq 1$  has been derived and is consistent with eq. (12). In this paper, for a small but suitable sample of spirals, we have derived the halo velocity profile over the *entire* stellar disk, with unprecedented precision.

The fact that, dark halo velocities rise linearly with radius from  $0.25R_D$  to  $\sim 3R_D$ , sets a serious upper limit to the dynamical relevance of CDM–like dark halos in spirals. In fact, let us assume, conservatively, 1) CDM halo velocities scale as:  $V_{CDM}(r) \propto r^{1/4}$ , 2) CDM halos coexist with constant–density halos, 3) the uncertainties on  $V_H(r)$  at innermost radii arise from the non–linearity of CDM halo velocities. Even with these most favourable assumptions, one gets:  $V_{CDM}^2(R_{opt}) < 0.05V_H^2(R_{opt})$  i.e. a negligible dynamical importance of a CDM halo in the optical regions.

Then, the claim by Burkert and Silk (1997) of a mass structure including a MACHO dark halo with cored velocity profile *and* a standard CDM halo meets a difficulty. In fact, from the argument above, the MACHO halos must make  $> 95\%$  of the dark mass inside  $R_{opt}$ , and even by assuming at this radius an abrupt density cut–off, the baryonic DM will still dominate the dynamics well beyond  $25 R_D$ . The CDM halos would have a dynamical importance only in regions so external (and not probed by kinematics) that their cosmological role is totally unclear.

## REFERENCES

- Begeman, K.G., Broeils, A.H. & Sanders, R.H. (1991) MNRAS, **249**, 523.  
 Blais-Ouellette, S., Carignan, C., Amram, P. & Coté, S. (1999) astro-ph/9911 223.  
 Burkert, A. (1995) ApJ, **447**, L25.  
 Burkert, A. & Silk, J. (1997) ApJ, **488**, L55.  
 Cole, S. & Lacey, C. (1997) MNRAS, **281**, 716.  
 Flores, R. & Primack, J.R. (1994) ApJ, **427**, L1.  
 Freeman, K.C., (1970) ApJ, **160**, 811F.  
 Fukushige, T. & Makino, J. (1997) ApJ, **477**, L9.  
 Gelato, S. & Sommer-Larsen, J. (1999) MNRAS, **303**, 321.  
 Ghigna, S., Moore, B., Governato, F., Lake, G., Quinn, T. & Stadel, J. (1999) preprint (astro-ph/9910166)  
 Jing, Y.P., (1999) ApJ, **515L**, 45J  
 Jing, Y.P. & Suto, Y. (1999) in press, (astro-ph/9909478)  
 Kravtsov, A.V., Klypin, A.A., Bullock, J.S., & Primack, J.R. (1998) ApJ, **502**, 48.  
 Martin, C.L. (1999) ApJ, **513**, 142.  
 Mathewson, D.S., Ford, V.L. & Buchhorn, M.K.C. (1992) ApJS, **81**, 413.  
 McGaugh, S.S., & de Block, W.J.G. (1998) ApJ, **499**, 41.  
 Moore, B. (1994) Nature, **370**, 629.  
 Moore, B., Governato, F., Quinn, T., Stadel, J., & Lake, G. (1998) ApJ, **499**, L5.  
 Navarro, J.F. (1996) ASP conf. **117**, 404 eds. M. Persic & P. Salucci  
 Navarro, J.F., Frenk, C.S. & White, S.D.M. (1996) ApJ, **462**, 563.  
 Navarro, J.F., Frenk, C.S. & White, S.D.M. (1997) ApJ, **490**, 493.  
 Nusser, A. & Sheth, R.K. (1999) MNRAS, **303**, 685N.  
 Persic, M. & Salucci, P. (1988) MNRAS, **234**, 131P.  
 Persic, M. & Salucci, P. (1990b) MNRAS, **245**, 577  
 Persic, M. & Salucci, P. (1992) Astro. Lett. Communications, **28**, 307.  
 Persic, M., Salucci, P. & Ashman, K.M. (1993) A&A, **279**, 343.  
 Persic, M. & Salucci, P. (1995) ApJS, **99**, 501.  
 Rhee, M.-H. & van Albada, T.S. (1996) A&AS, **115**, 407R.

- Salucci, P. (1997) ASP Conference Series, **117**  
Salucci, P. (1999) MNRAS submitted  
Salucci, P., Ratnam, C., Monaco P., Danese, L., (1999) MNRAS in press, (astro-ph/9812485)  
Salucci, P. & Burkert, A. (1999) ApJ submitted  
Salucci, P. & Persic, M. (1999a) MNRAS, **309**, 923  
Stil, J. (1999) Ph.D. Thesis, Leiden University  
Swaters, (1999) Ph.D. Thesis, Groningen University  
Tissera, P.B. & Dominguez-Tenreiro, R. (1998) MNRAS, **297**, 177  
Tormen, G., Bouchet, F.R. & White, S.D.M. (1997) MNRAS, **286**, 865  
van Albada, T.S., Bahcall, J.S., Begeman, K. & Sancisi, R. (1985) ApJ, **295**, 305  
van den Bosch, F.C., Robertson, B.E., Dalcanton, J. & de Blok, W.J.G. (1999) astro-ph/9911372  
Verheijen, M.A.W. (1997), Ph.D. Thesis (Cap. 6), Groningen University